



**"Gheorghe Asachi" Technical University of Iasi, Romania**



---

## **HYDROGEOCHEMISTRY AND ENVIRONMENTAL ISOTOPE COMPOSITIONS AND THEIR EVOLUTION IN GEOTHERMAL GROUNDWATER IN YIZHANG, HUNAN PROVINCE, CHINA**

**Junjie Ba<sup>1</sup>, Chuntian Su<sup>1\*</sup>, Qiuju Chen<sup>2</sup>, Xiaodong Pan<sup>1</sup>**

<sup>1</sup>*Institute of Karst Geology, CAGS/Key Laboratory of Karst Dynamics, MNR&GZAR, Guilin 541004, China*

<sup>2</sup>*School of Environmental Studies, China University of Geosciences (Wuhan), Wuhan 430074, China*

---

### **Abstract**

Yizhang, located in south of Hunan province of China is rich in geothermal resources. This paper aimed to study the concentrations of cations, e.g., K<sup>+</sup>, Ca<sup>2+</sup>, Na<sup>+</sup>, Mg<sup>2+</sup> and conducted the analysis of the environmental isotope characteristics of δD, δ<sup>18</sup>O and δ<sup>13</sup>C. Further there are explained the rules of the generation and evolution of geothermal groundwater in Yizhang. The temperature of geothermal groundwater in Yizhang was between 34.2 and 45.4 °C, with a neutral pH and a high electrical conductivity. The hydrogeochemical characteristics changed in the order HCO<sub>3</sub>-Ca, HCO<sub>3</sub>-Ca, HCO<sub>3</sub>-SO<sub>4</sub>-Ca, SO<sub>4</sub>-Ca-Mg corresponding to surface water-underground cold water-Yongkou hot springs-Yiliu hot springs in Yizhang area. Compared with that in Yongkou area, the water-rock interaction of groundwater lasted for a longer time in a more enclosed environment in Yiliu area. The δD-δ<sup>18</sup>O isotope analysis showed that the geothermal groundwater was generated from atmospheric rainfall and the recharge height of geothermal field was between 695~1040m. The δ<sup>13</sup>C isotope analysis demonstrated that the CO<sub>2</sub> generated during water-rock interactions was induced by factors of biogenetic, atmosphere, mantle and carbonate rocks degeneration. The result of this study was that the geothermal groundwater in Yongkou and Yiliu was formed from the same thermal resource in the same environment. Our research contributed to the determination of the border of geothermal groundwater fields, the modelling of the geological thermal reservoir structure, and the environmental evaluation of the groundwater in Yizhang, Hunan province, China.

**Keywords:** hot springs, environmental isotope, hydrogeochemistry, Yizhang, China

*Received: August, 2018; Revised final: November, 2018; Accepted: December, 2018; Published in final edited form: March, 2019*

---

### **1. Introduction**

Large number of studies and exploitations of geothermal resources are focused on medium-high temperature geothermal fields (Barbato et al., 2018). With the shortage of fossil energy and the increasing demand of clean energy, it is more and more urgent to exploit the medium-low temperature geothermal sources (Caldera et al., 2018; Guo et al., 2014; Wang, 1996). Fundamental studies on the groundwater hydrogeochemistry, environmental isotope characteristics analysis, origin and causes of geotherms, are key tools to guide the study and the exploitation of the medium-low temperature

geothermal sources (Cannistraro et al., 2018; Wang et al., 2008; Xu, 2009).

In recent years, environmental isotope technology has been a unique and irreplaceable way to study the underground water resources and the environmental issues, which helps to explain the mechanism of water movement from both macro and micro aspects (Wang et al., 2017; Zaher et al., 1997). The hydrodynamic conditions and the evolution models of the geothermal groundwater can be obtained from the comparison of the δD, δ<sup>18</sup>O and δ<sup>13</sup>C and the hydrochemical characteristics (Du et al., 2005). More specifically, isotope characteristics analysis, chemography and statistical analysis are

---

\* Author to whom all correspondence should be addressed: e-mail: suchuntian@karst.ac.cn

useful tools to study the water-rock interactions, groundwater circulation time, runoff process, geotherm generation conditions (Bakari et al., 2005; Majumdar et al., 2009; Rissmann et al., 2012).

Researches of Yizhang geothermal fields were mainly on the development models so far. No systematic analysis has been taken to study the hydrogeochemical and environmental isotope characteristics. The main purpose of this paper was to study the hydrogeological conditions of geothermal fields, and to establish a model of integrated hydrogeochemical characteristics, environmental factors and their evolution laws in Yizhang area.

## 2. Geological setting

Yizhang County is located in the south of Chenzhou City, Hunan, China,  $24^{\circ}53' - 25^{\circ}41'N$  and  $112^{\circ}37' - 113^{\circ}20'E$  (Fig. 1a). The main geomorphologic shape in Yizhang is eroded hilly landforms and the terrain is undulating. The highest peak is Qitianling, with an altitude of 1654 meters above sea level (MASL) in the northwest direction and the lowest is the Zhangshui River, which is less than 194 MASL. Yizhang is in the climate transition zone from subtropical zone to temperate zone, which brings that the perennial mean temperature is  $18.3^{\circ}C$ ; the perennial mean precipitation is 1495.0 mm; and the perennial mean evaporation is 1436.0 mm.

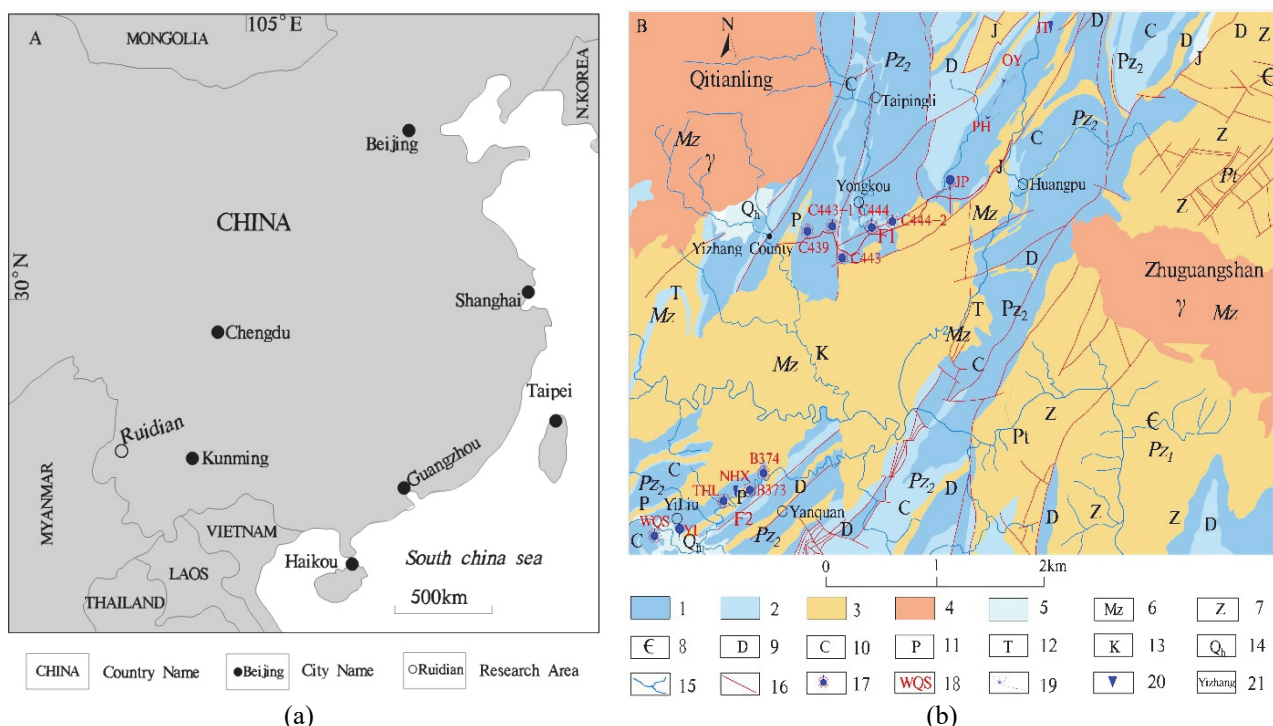
The Stratum of Yizhang contains many layers. The exposed stratum includes Cambrian, Devonian, Carboniferous, Jurassic and Quaternary Periods, with

Silurian lacuna and Ordovician lacuna. Therefore, Indosinian ( $\gamma_5^1$ ) and Yanshanian ( $\gamma_5^2$ ) magmatic rocks can be found in Qitianling and Zhuguangshan, respectively. The complex geological structures mainly generate NNE-NE-trending and nearby NS-trending structure, and secondarily generate NW-trending structure, as shown in Fig. 1b.

## 3. Hydrochemical characteristics analysis

### 3.1. Main chemical characteristics

There are two main hot spring areas in Yizhang, named Yongkou and Yiliu (Fig. 1b). The concentrations (unit: mg/L) of main ions ( $K^+$ ,  $Na^+$ ,  $Ca^{2+}$ ,  $Mg^{2+}$ ,  $HCO_3^-$ ,  $SO_4^{2-}$ ,  $Cl^-$ ) in the samples of the Yizhang hot springs are shown in Table 1. In the Fig. 2, it was found that the  $Ca^{2+}$  concentration was the highest in all samples-about 80% of the cations. The concentration of  $Mg^{2+}$  was the second highest, lower than 10% in all the cations in the surface water and underground cold water. The  $Mg^{2+}$  concentration in samples from Yongkou hot spring (No. C439, C443-1, C443, C444, C444-2) and Yiliu hot spring (No. WQS, THL, B373, B374) was approximate 15% and 25%, respectively. The overall  $Na^+$  and  $K^+$  concentration was lower than 10% in all samples. The location distribution of the sampling points in the study area was shown in Fig. 1b. In Fig. 2, the  $Cl^-$  concentration was lower than 5% in all samples. The  $HCO_3^-$  concentration was approximate 90% of all the anions in surface water and underground cold water.

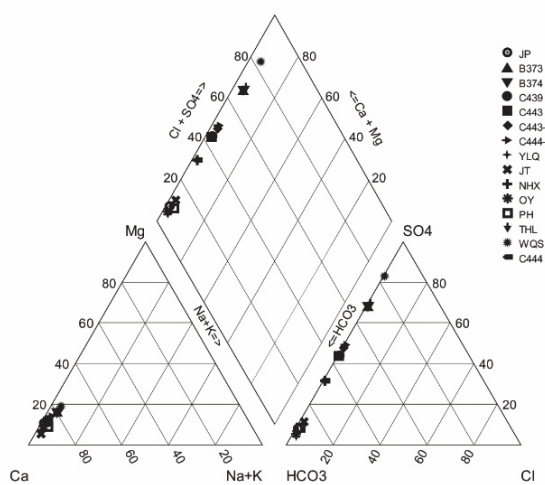


**Fig. 1. (a)** Location of the Yizhang; **(b)** Sampling sites in the Yizhang geothermal fields: 1-Carbonate area, 2-Impure carbonate zone; 3-Sand-shale zone; 4-Mesozoic Granite area; 5-Cenozoic Quaternary; 6-Mesozoic; 7-Proterozoic Sinian system; 8-Palaeozoic Cambrian system; 9-Palaeozoic Devonian system; 10- Palaeozoic Carboniferous system; 11- Palaeozoic Permian system; 12- Mesozoic Triassic systems; 13- Mesozoic Cretaceous system; 14- Cenozoic Quaternary; 15-River; 16-fault; 17-Hot spring; 18-Sample number; 19-Underground water; 20-Surface water; 21-Research area

**Table 1.** Basic features and major compositions of spring and river waters from the Yizhang geothermal areas

Sampling site	No.	T (°C)	EC $\mu\text{s}/\text{cm}$	PH	K <sup>+</sup>	Na <sup>+</sup>	Ca <sup>2+</sup>	Mg <sup>2+</sup>	Cl <sup>-</sup>	SO <sub>4</sub> <sup>2-</sup>	HCO <sub>3</sub> <sup>-</sup>	SiO <sub>2</sub>	F
					mg/L	mg/L	mg/L	mg/L	mg/L	mg/L	mg/L	mg/L	mg/L
Yongkou Hotspring	C439	42.9	748	7.4	4.61	2.59	156.0	12.08	1.88	180.6	294.6	37.0	0.60
	C443-1	43.5	781	7.3	5.38	2.86	161.2	12.88	1.87	205.7	286.2	40.9	0.67
	C443	41.5	770	7.0	4.82	2.66	152.7	11.99	1.86	179.8	294.6	37.8	0.62
	C444	43.5	675	7.2	3.08	2.18	139.0	10.74	2.08	114.1	315.0	36.7	0.44
	C444-2	42.9	763	6.9	5.42	2.79	156.2	15.40	1.66	207.1	270.9	44.2	0.72
Yiliu Hotspring	WQS	45.4	1574	6.6	8.88	17.12	330.5	48.72	2.68	821.4	216.7	43.0	2.57
	THL	42.7	1074	7.0	6.15	11.72	213.1	28.12	4.98	427.8	233.7	31.6	1.40
	B373	34.2	1123	7.4	4.97	10.77	218.2	26.86	3.87	440.2	257.4	27.2	1.18
	B374	32.9	1127	7.4	4.81	10.55	217.1	26.64	3.70	431.7	250.6	26.7	1.19
Under-ground water	PH	18.5	350	7.3	3.74	1.48	69.1	3.98	2.74	15.4	216.7	5.5	0.10
	JP	18.0	373	7.5	0.95	0.86	75.4	5.38	1.84	14.6	225.21	5.5	0.09
	YLQ	20.5	485	7.2	1.52	2.44	100.9	4.66	3.59	9.8	291.25	7.1	0.07
Surface water	NHX	18.7	252	7.3	3.07	2.18	140.5	10.79	2.04	114.9	318.34	10.5	0.43
	JT	17.0	363	7.9	2.01	1.51	76.9	2.59	2.72	21.1	209.97	5.7	0.10
	OY	16.8	352	7.8	1.46	0.85	73.1	4.44	1.94	9.5	226.90	5.0	0.09

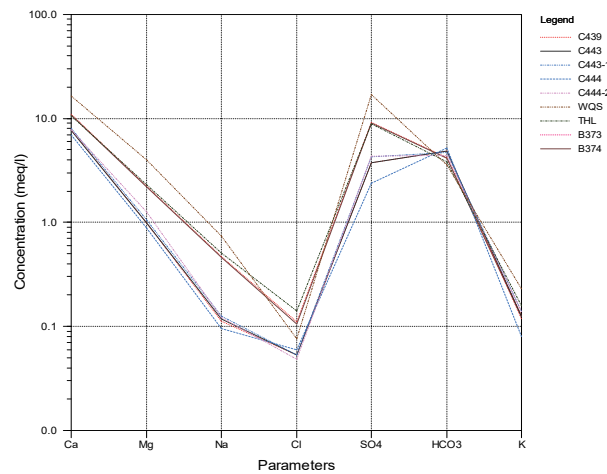
However, the anions characteristics in Yongkou hot spring and Yiliu hot spring were different. The concentrations of HCO<sub>3</sub><sup>-</sup> + CO<sub>3</sub><sup>2-</sup> and SO<sub>4</sub><sup>2-</sup> were nearly the same in Yongkou hot spring sample, both were about 50% of the anions, while the SO<sub>4</sub><sup>2-</sup> concentration was turned out to be about 80% in Yiliu hot spring sample (Fig. 2).

**Fig. 2.** Piper triangle diagram of ions

According to the above analysis, the following conclusion can be obtained that the hydrogeochemical characteristics changed in the order "HCO<sub>3</sub>-Ca→HCO<sub>3</sub>-Ca→HCO<sub>3</sub>-SO<sub>4</sub>-Ca→SO<sub>4</sub>-Ca-Mg" corresponding to surface water (No. NHX, JT, OY) – underground cold water (No. PH, JP, YLQ) – Yongkou hot springs (No. C439 to No. C444-2) – Yiliu hot springs (No. WQS to No. B374) respectively in Yizhang area. In addition, the electrical conductivity increased successively.

The main anions were HCO<sub>3</sub><sup>-</sup> and Cl<sup>-</sup>. Also, the interaction between underground cold water and the runoff geothermal groundwater became weak, and the geothermal system was enclosed to some extent. The temperature of surface water (hot spring) was relatively high.

Fig. 3 was the Schoeller plot for different samples, which was performed by AquaChem software. In Fig. 3, it was found that the hydrochemical characteristics in Yongkou hot spring area and Yiliu hot spring area were almost the same. Therefore, both hot springs were sharing the same thermal resource, and had been formed in the same environment.

**Fig. 3.** Schoeller plot for different samples

### 3.2. Correlation analysis of the main ions

Farnham et al. (2002) and Kuells et al. (2000) thought Cluster Analysis was a suitable method for the comprehensive consideration of hydrochemical compositions. Cluster Analysis can present the supply sources of the geothermal groundwater and/or the hot springs, hydraulic connections and the interaction between geothermal fluid and the environment (Glavan et al., 2015; Ternik et al., 2018). The Q-type Cluster Analysis was applied in SPSS software to investigate the concentration of main ions and natural abundance of trace elements in samples. The Q-type Cluster Analysis tree diagram is shown in Fig. 4. Based on the distance coefficient <15, all 15 samples were divided into two types:

(1) Samples from the hot spring area in Yiliu, contained relatively high concentration of ions and abundance value of trace elements, which was caused by the development of large fault zone and secondary fault zone.

(2) Samples from the hot spring area in Yongkou, contained the lowest concentration of ions and abundance value of trace elements.

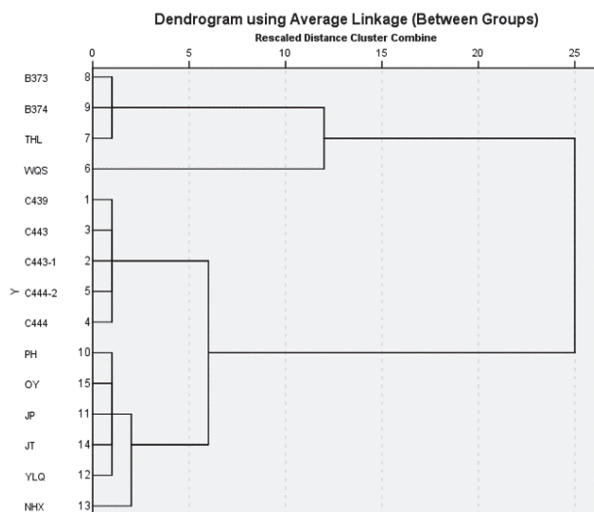


**Fig. 4.** Q-type Cluster Analysis tree diagram

This division captured the relationship of hydrochemical characteristics from different monitoring time. The monitoring sites were classified as the same sub-cluster if there was little difference in temperature of samples.

The statistical result of the Q-type Cluster Analysis above was in accordance with the real geothermic geological distribution characteristics in Yizhang geothermal fields in a better way. Therefore, Q-type Cluster Analysis can be used to analyze the hydrochemical characteristics of geothermal fluids.

Correlation analysis could be applied to study the similarity and/or difference of the supply resources and the hydrochemical characteristics of geothermal fluids (Helstrup et al., 2007; Yidana et al., 2008). SPSS software was used for the analysis of the correlation among the main ions in geothermal fluid samples, which could be further used to analyse the water-rock interaction.

The correlation of different ions was shown in Table 2. Regarding to the correlation with temperature (T), it was found that only pH and the  $\text{HCO}_3^-$  anion are negative. The electrical conductivity (EC) and other ions all had positive correlation with temperature, which was due to the medium-low temperature of Yizhang geothermal groundwater. Despite pH, all ions had very close positive correlation with EC, especially  $\text{Ca}^{2+}$ ,  $\text{Mg}^{2+}$ ,  $\text{Na}^+$ ,  $\text{K}^+$  and  $\text{SO}_4^{2-}$ , with corresponding correlation coefficient (R) of 1.00, 1.00, 0.98, 0.94 and 1.00, respectively. The electrical conductivity reflected the water-rock interaction and in return the water-rock interaction controlled the electrical conductivity of the water.

### 3.3. Water-Rock interactions and the mineral saturation index

The concentration of  $\text{Na}^+$ ,  $\text{K}^+$  and  $\text{Mg}^{2+}$  was depicted in the Na-K-Mg triangle diagram (Fig. 5a), which was created by Giggenbach (1994). In Fig. 5a, it was found that all the samples were located at bottom right corner in the triangle diagram, which indicated that the water-rock interaction in Yizhang geothermal groundwater was in its infancy stage.

This paper applied PHREEQC to calculate the mineral saturation indexes of the minerals in the geothermal groundwater. The mineral saturation index (SI) plots were shown in Fig. 5b. In Fig. 5b, it was found that the SIs of Dolomite, Calcite, Chalcedony and Quartz were above 0, which demonstrated that the Dolomite, Calcite, Chalcedony and Quartz were saturated whereas other minerals were not saturated in the geothermal groundwater. Quartz were saturated whereas other minerals were not saturated in underground cold water and surface water, as listed in Table 3. In Table 3, it was also found that the SIs of Gypsum and Fluorite increased from Yongkou hot spring to Yiliu hot spring, which demonstrated that the Gypsum and Fluorite dissolved during this flowing process.

Chalcedony and Quartz were saturated in the thermal groundwater, which implied that the increase of temperature prompted the dissolution of  $\text{SiO}_2$ . In addition, the SIs of other minerals in Yiliu hot spring were higher than those in Yongkou hot spring, which showed that the geothermal sources of Yiliu were more abundant than those of Yongkou area.

**Table 2.** Correlation analysis of the main ions in geothermal fluid samples

	<b>EC</b>	<b>pH</b>	<b><math>\text{Ca}^{2+}</math></b>	<b><math>\text{Mg}^{2+}</math></b>	<b><math>\text{Na}^+</math></b>	<b><math>\text{K}^+</math></b>	<b><math>\text{HCO}_3^-</math></b>	<b><math>\text{SO}_4^{2-}</math></b>	<b><math>\text{Cl}^-</math></b>	<b>T</b>
EC	1.00	-0.80	1.00	1.00	0.98	0.94	-0.91	1.00	0.46	0.52
pH		1.00	-0.79	-0.80	-0.77	0.78	-0.80	-0.80	-0.32	-0.44
$\text{Ca}^{2+}$			1.00	0.99	-0.96	0.94	-0.89	1.00	0.41	0.52
$\text{Mg}^{2+}$				1.00	0.98	0.93	-0.92	1.00	0.48	0.50
$\text{Na}^+$					1.00	0.89	-0.94	0.97	0.64	0.44
$\text{K}^+$						1.00	-0.93	0.95	0.36	0.77
$\text{HCO}_3^-$							1.00	-0.92	-0.64	-0.67
$\text{SO}_4^{2-}$								1.00	0.45	0.54
$\text{Cl}^-$									1.00	0.07
T										1.00

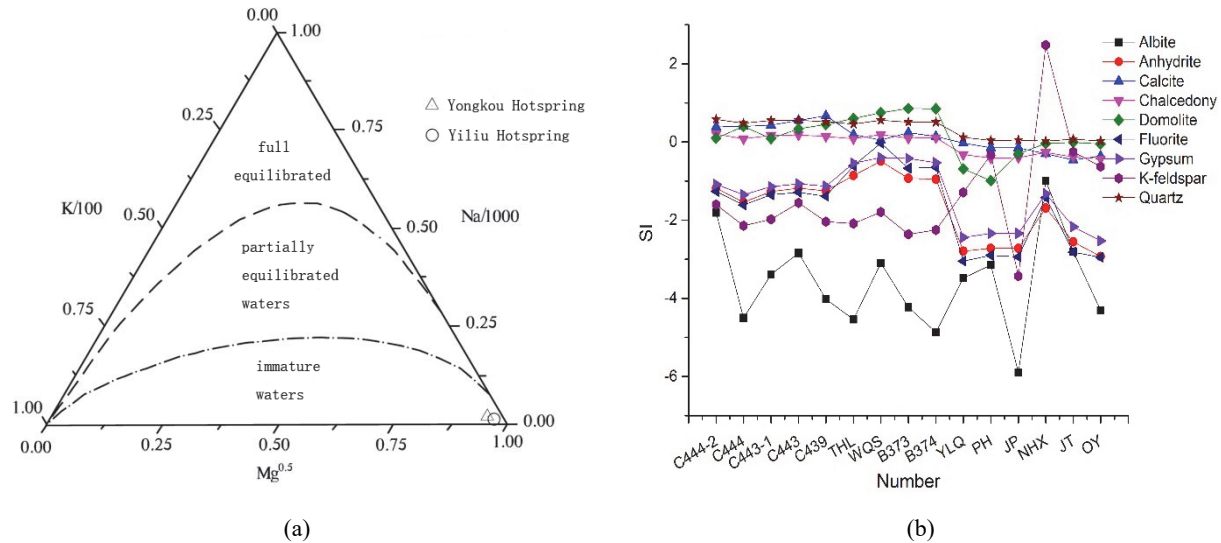


Fig. 5. (a)Na-K-Mg triangle diagram; (b) Mineral saturation indexes plot

Table 3. Mineral saturation indexes of waters in Yizhang area

Number	Albite	Anhydrite	Calcite	Chalcedony	Dolomite	Fluorite	Gypsum	K-feldspar	Quartz
C444-2	-1.81	-1.18	0.39	0.20	0.10	-1.26	-1.08	-1.60	0.58
C444	-4.50	-1.54	0.40	0.08	0.40	-1.61	-1.35	-2.14	0.48
C443-1	-3.39	-1.27	0.43	0.17	0.09	-1.35	-1.14	-1.98	0.55
C443	-2.84	-1.18	0.55	0.18	0.34	-1.29	-1.07	-1.56	0.56
C439	-4.02	-1.25	0.67	0.14	0.45	-1.39	-1.13	-2.04	0.52
THL	-4.54	-0.86	0.19	0.08	0.60	-0.61	-0.54	-2.09	0.46
WQS	-3.10	-0.49	0.05	0.19	0.75	-0.03	-0.40	-1.79	0.56
B373	-4.23	-0.93	0.24	0.10	0.86	-0.67	-0.42	-2.36	0.51
B374	-4.87	-0.95	0.14	0.11	0.85	-0.65	-0.53	-2.25	0.51
YLQ	-3.48	-2.79	-0.03	-0.32	-0.69	-3.05	-2.44	-1.29	0.12
PH	-3.15	-2.72	-0.15	-0.41	-0.99	-2.90	-2.34	-0.33	0.04
JP	-5.90	-2.72	-0.15	-0.40	-0.30	-2.94	-2.34	-3.43	0.05
NHX	-0.99	-1.69	-0.30	-0.27	-0.04	-1.42	-1.32	2.48	0.02
JT	-2.81	-2.56	-0.46	-0.38	-0.01	-2.82	-2.17	-0.25	0.07
OY	-4.31	-2.93	-0.36	-0.43	-0.05	-2.95	-2.53	-0.63	0.03

The concentration of SiO<sub>2</sub> in underground cold water and surface water was much lower than that in geothermal groundwater. The concentration of SiO<sub>2</sub> in the geothermal groundwater is between 30 and 50 mg/L, while it was lower than 10 mg/L in the underground cold water. The positive correlation between temperature and SiO<sub>2</sub> concentration showed that the dissolution in Feldspar, Chalcedony and Quartz would increase with the temperature.

However, the impact of the increase of SiO<sub>2</sub> concentration was different on the SIs of the minerals. Fig. 6 presented that with the increase of SiO<sub>2</sub> concentration, the SIs of Na-Feldspar and K-Feldspar increased most rapidly, whereas the SIs of Chalcedony and Quartz almost stayed the same. This result showed that the SiO<sub>2</sub> in the geothermal groundwater were basically dissolved in Feldspar while the dissolution was not obvious in Chalcedony and Quartz.

#### 3.4. As, Sb and other trace elements in hot spring waters

The concentration of trace elements in hot springs and surface waters was given in Table 4. The spring waters in Yongkou area showed higher concentration of Al, As, and Hg (0.6–177.0 µg/L, 4.53–9.53 µg/L and 1.13–36.6 µg/L, respectively), whereas the spring waters in Yiliu area presented higher concentration of Sr, Zn, Co, Cu and Ni (3332–6254 µg/L, 0.8–2.69 µg/L, 0.8–1.27 µg/L, 1.82–2.29 µg/L and 11.4–18.0 µg/L, respectively).

The concentration of As in Yongkou (4.53–9.53 µg/L) and Yiliu hot springs (2.63–6.36 µg/L) (Table 4) was much higher than that in the underground cold water (0.09–1.47 µg/L) and surface water (0.76–1.89 µg/L). This was due to the leaching of as after the water-rock interaction.

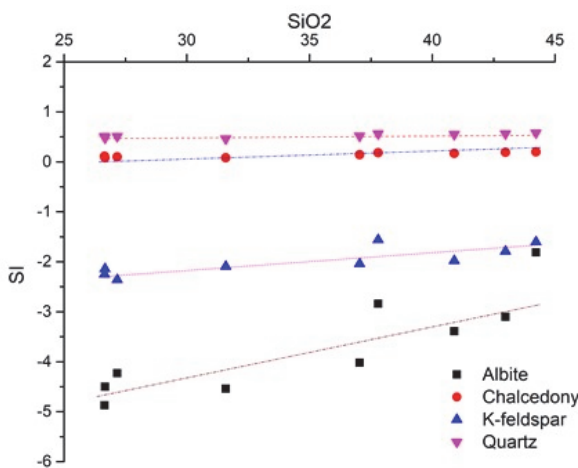


**Fig. 6.** Saturation indexes of Albite, Chalcedony, K-feldspar and Quartz vs. the concentration of SiO<sub>2</sub>

### 3.5. Potential environmental impact of hot springs

We investigated the heavy metals concentration in hot springs, and the water quality turned out to be overall good. The hot springs, as geothermal resources, could be fairly exploited. Furthermore, Yiliu hot springs were in rich of Sr (3332–6254 µg/L), which was helpful to the human's bones and teeth growth. Therefore, geothermal fields in Yiliu area can be exploited as rich Sr fields.

The presence of toxic elements such as arsenic and manganese in soils, surface and groundwater are of great concern (Nimick et al., 1998). In both the Yongkou and Yiliu geothermal fields all the spring waters have arsenic contents that are significantly lower than the 10 µg/L guideline set by the World Health Organization (WHO, 1993). Among all hot spring sampling sites, the C443-1 hot spring has the highest As content, which was 9.53 µg/L, and the THL hot spring has the highest As content (2.63 µg/L). The manganese content of the NHX water sample (214 µg/L) in the surface water sample is much larger than the detection value of other water samples. Such high manganese values may be related to the mining of manganese ore around the sampling point.

**Table 4.** Trace element concentrations (µg/L) of spring and surface waters of Yizhang area

Number	Al	Cu	Pb	Zn	Cr	Ni	Co	Cd	Mn	As	Hg	Sr
C439	<0.6	0.50	<0.07	<0.8	2.79	9.21	0.57	<0.06	0.80	8.84	17.20	750
C443-1	166.0	0.79	0.86	<0.8	1.52	9.81	0.85	<0.06	28.0	9.53	23.20	840
C443	<0.6	0.57	<0.07	<0.8	2.67	9.16	0.58	<0.06	<0.06	6.80	1.13	768
C444	<0.6	0.29	<0.07	<0.8	3.07	7.52	0.48	<0.06	1.87	4.53	36.60	503
C444-2	177.0	0.63	0.25	<0.8	2.62	9.32	0.75	<0.06	7.30	7.28	0.39	905
WQS	<0.6	1.82	<0.07	<0.8	1.52	18.0	1.27	<0.06	12.3	6.36	0.72	6254
THL	6.7	1.36	<0.07	2.69	1.63	11.4	0.80	<0.06	1.25	2.63	12.10	3332
B373	4.6	2.20	0.58	1.02	4.06	13.3	1.14	<0.06	1.37	4.85	<0.07	3766
B374	3.8	2.29	0.60	0.83	3.94	13.0	1.15	<0.06	0.43	4.86	<0.07	3710
PH	178.0	0.80	4.63	2.88	1.85	4.46	0.35	<0.06	25.0	1.47	1.27	80.3
JP	<0.6	<0.09	<0.07	<0.8	3.61	4.38	0.21	<0.06	<0.06	<0.09	0.12	86.5
YLQ	33.1	<0.09	<0.07	<0.8	2.83	6.19	0.38	<0.06	1.51	<0.09	19.3	170.0
NHX	1368.0	2.89	7.40	12.0	3.48	5.01	1.26	0.14	214	0.76	0.93	68.5
JT	276.0	1.44	1.15	5.13	1.65	7.34	1.38	<0.06	54.3	1.12	0.60	97.6
OY	215.0	0.55	1.80	<0.8	1.80	4.74	0.41	<0.06	30.7	1.89	1.84	34.3

The existing hot springs generally have good water quality and should be protected. It should avoid human, cattle and poultry excrement mixed into hot spring water.

### 4. Environmental isotope characteristics analysis

#### 4.1. $\delta^{18}\text{O}$ and $\delta\text{D}$ characteristics

In this study, 16 water samples were collected for  $\delta^{18}\text{O}$  and  $\delta\text{D}$  characteristics analysis: 5 from Yongkou hot spring, 4 from Yiliu hot spring, 3 from surface water, 3 from underground cold water and 1 from rainwater. The analytical and test data values of  $\delta^{18}\text{O}$  and  $\delta\text{D}$  in different samples were listed in Table 5. The average ratios of  $\delta^{18}\text{O}$  in Yongkou and Yiliu hot spring were  $-5.88\text{\textperthousand}$  and  $-5.97\text{\textperthousand}$ , respectively. The average ratios of  $\delta\text{D}$  in Yongkou and Yiliu hot spring were  $-37.38\text{\textperthousand}$  and  $-38.44\text{\textperthousand}$ , respectively. In addition, the average ratios of  $\delta^{18}\text{O}$  and  $\delta\text{D}$  in surface water were  $-7.22\text{\textperthousand}$  and  $-46.18\text{\textperthousand}$ , respectively. The average ratios of  $\delta^{18}\text{O}$  and  $\delta\text{D}$  in rainwater were  $-10.84\text{\textperthousand}$  and  $-76.58\text{\textperthousand}$ , respectively.

Generally speaking, the  $\delta^{18}\text{O}$  and  $\delta\text{D}$  isotopic composition gradually depleted from north to south in geothermal groundwater. The  $\delta^{18}\text{O}$  and  $\delta\text{D}$  isotopic composition in surface water was higher than that of underground cold water, which was due to the effect of evaporation. The  $\delta^{18}\text{O}$  and  $\delta\text{D}$  isotopic composition in geothermal groundwater, underground cold water and surface water was higher than that of present-day rainwater.

#### 4.2. Supply source of hot spring and $\delta^{18}\text{O}$ characteristics

According to the comparison of  $\delta^{18}\text{O}$  and  $\delta\text{D}$  isotopic composition in the geothermal groundwater with global atmospheric rainfall line or local atmospheric rainfall line, it can be determined that the geothermal source is seawater, magmatic water, rainfall, and so on (Ghasemkhani et al., 2018; Portugal et al., 2005). The global atmospheric rainfall line equation was shown as follows (Eq. 1) (Craig, 1963):

**Table 5.**  $\delta^{18}\text{O}$  and  $\delta\text{D}$  characteristics in the samples of Yizhang waters

<i>Number</i>	$\delta^{18}\text{O}_{(\text{V-SMOW})} \text{\%}$	<i>Average value</i>	$\delta\text{D}_{(\text{V-SMOW})} \text{\%}$	<i>Average value</i>
C444-2	-6.23	-5.88	-37.82	-37.38
C444	-5.72		-38.08	
C443	-6.07		-38.52	
C443-1	-6.12		-37.3	
C439	-5.28		-35.19	
B374	-6.26	-5.97	-38.19	-38.44
B373	-5.82		-38.76	
THL	-5.71		-37.89	
WQS	-6.09		-38.94	
YLQ	-6.59	-7.28	-49.86	-46.85
PH	-7.94		-49.88	
JP	-7.31		-40.81	
JT	-7.58	-7.22	-38.66	-46.18
OY	-7.66		-52.89	
NHX	-6.42		-46.99	
Rainwater	-10.84	-10.84	-76.58	-76.58

$$\delta\text{D} = 8\delta^{18}\text{O} + 10 \quad (1)$$

Zheng et al (1983) studied the isotopic composition of in Changsha, China, and gave the atmospheric rainfall line equation in Changsha (Eq. 2):

$$\delta\text{D} = 8.47\delta^{18}\text{O} + 15.46 \quad (2)$$

Since Yizhang is close to Changsha and share the same climate with Changsha, the (Eq. 2) is used for the analysis of the  $\delta^{18}\text{O}$  and  $\delta\text{D}$  isotopic composition in Yizhang area. Comparing the  $\delta^{18}\text{O}$  and  $\delta\text{D}$  in the 16 samples with the (Eq. 1) and (Eq. 2), it was found that the isotopic compositions in geothermal groundwater, underground cold water and surface water kept in line with (Eq. 1) and (Eq. 2), as shown in Fig. 7. Therefore, rainwater was the supply source of geothermal groundwater, which formed by deep circulation under heating.

The surface water sample was slightly drifted from Changsha atmospheric rainfall line (Fig. 7), which indicated that the  $\delta^{18}\text{O}$  and  $\delta\text{D}$  in surface water were enriched after evaporation process. The underground cold water sample was located on the Changsha atmospheric rainfall line, which indicated that the supply source of the underground cold water was rainwater and the supply source of the underground cold water was rather short so it circulated very fast. The  $\delta^{18}\text{O}$  and  $\delta\text{D}$  in hot springs were more negative than underground cold water, so it was inferred that the supply source of hot springs was some area with high altitude.

From Fig. 8, it was found that the  $\delta^{18}\text{O}$  in hot springs had positive drift to some extent. This was mainly due to the water-rock interaction. In order to explain this drift,  $d$  was defined to calculate the excess of  $\delta\text{D}$  (Eq. 3):

$$d = \delta\text{D} - 8\delta^{18}\text{O} \quad (3)$$

From Fig. 8, it was found that the  $\delta^{18}\text{O}$  in hot springs had positive drift to some extent. This was mainly due to the water-rock interaction. In order to

explain this drift,  $d$  was defined to calculate the excess of  $\delta\text{D}$  (Eq. 3):

$$d = \delta\text{D} - 8\delta^{18}\text{O} \quad (3)$$

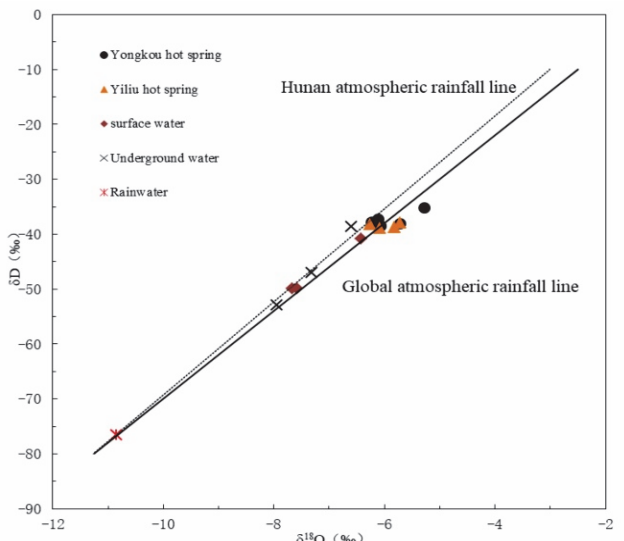


**Fig. 7.** The relationship between the  $\delta^{18}\text{O}$  and  $\delta\text{D}$  isotopic composition in samples and global atmospheric rainfall line and local atmospheric rainfall line

In this formula,  $d$  can be used to index the water-rock interaction extend. With the decreasing of  $d$ , it indicated that the hot spring was farther from its supply source. The runoff path was longer in an enclosed geological environment and the water-rock interaction was stronger. Fig. 8 depicted that the  $d$  of Yongkou hot spring was slightly lower than that of Yiliu hot spring, which means Yiliu hot spring was farther from its supply source; the runoff path was longer in a more enclosed geological environment; and the water-rock interaction was stronger than Yongkou hot spring.

The hydrogen and oxygen isotope composition of atmospheric rainfall has an elevation effect, which recharge elevation and recharge area of groundwater can be determined.

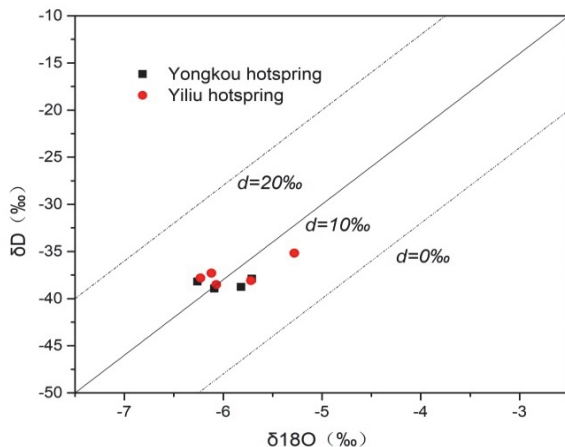


**Fig. 8.** The  $\delta^{18}\text{O}$  and  $\delta\text{D}$  isotopic composition and the distribution of  $d$

$$H = H_r + (D - D_r)/\text{grad}D \quad (4)$$

In this (Eq. 4),  $H$ —the geothermal recharge area elevation, m;  $H_r$ —the isotope ratio in the air, m;  $D$ —the  $\delta\text{D}$  value of recharge water, ‰;  $D_r$ —the  $\delta\text{D}$  value of geothermal water, ‰;  $\text{Grad } D$ —the decreasing gradient with elevation, ‰/100m.

The  $\text{grad } D$  can be obtained from the  $\delta\text{D}$  values of two surface water samples of the Jiantian Reservoir and Nanhua River in the study area. The difference of  $\delta\text{D}$  between Jiantian Reservoir and Nanhua River water sample was  $-9.05\text{‰}$ , and the actual height difference was 521m. The calculated  $\text{grad } D$  value of regional atmospheric rainfall was  $-1.73\text{‰}/100\text{m}$ . The Ouyang water sample was replenished by atmospheric rainfall, then this point was selected as the  $\delta\text{D}$  value of the recharge water, and its  $\delta\text{D}$  value was  $-49.88\text{‰}$ . Substitution formula:

$$H = H_r + (-49.88\text{‰} - D_r) \times 100 / (-1.73\text{‰}) \quad (5)$$

The  $\delta\text{D}$  range of the Yongkou hot spring was  $-35.2\text{‰} \sim -38.5\text{‰}$ , which was substituted into the (Eq. 5), and the elevation of the hot spring supply was 847~1040m. The range of  $\delta\text{D}$  of the Yiliu hot springs was  $-37.9\text{‰} \sim -39.0\text{‰}$ , and the recharge elevation of Yiliu hot springs was 695~984m. The elevation of underground hot water supply in the two areas was similar, and it is consistent with the elevation of the regional northeast to the exposed carbonate area. It was confirmed that the source of underground hot

water supply in Yizhang area was the northeastward exposed carbonate area.

#### 4.3. Supply source of C in hot spring and $\delta^{13}\text{C}$ characteristics

Since the pH of hot spring water was in the range of 6.60~7.40,  $\text{HCO}_3^-$  was the main form of C in the water. Therefore, we analyzed  $\delta^{13}\text{C}_{\text{HCO}_3^-}$  ( $\delta^{13}\text{C}$ ) as the main  $\delta^{13}\text{C}$  characteristics. Isotope equilibrium between water and air complies with thermodynamics equilibrium. The supply source of  $\text{HCO}_3^-$  and  $\text{CO}_2$  can be confirmed quantitatively by calculating the equilibrium  $\delta^{13}\text{C}$  of  $\text{CO}_2$  and  $\text{HCO}_3^-$  contained in samples (Kim et al., 1997). When isotope exchange reaction reaches equilibrium, the relationship between  $\delta^{13}\text{C}_{\text{HCO}_3^-}$  and  $\delta^{13}\text{C}_{\text{CO}_2}$  was shown as follows (Eq. 6):

$$\delta^{13}\text{C}_{\text{HCO}_3^-} - \delta^{13}\text{C}_{\text{CO}_2} = -4.54 + 1.99 \times 10^6 / T^2 \quad (6)$$

In this formula,  $\delta^{13}\text{C}_{\text{HCO}_3^-}$  was the isotope ratio in the water;  $\delta^{13}\text{C}_{\text{CO}_2}$  was the isotope ratio in the air;  $T$  was the absolute temperature. Under the isotope equilibrium, the  $\delta^{13}\text{C}_{\text{HCO}_3^-}$  and  $\delta^{13}\text{C}_{\text{CO}_2}$  in geothermal groundwater were listed in Table 6. The  $\delta^{13}\text{C}_{\text{HCO}_3^-}$  in groundwater was in the range from  $-4.8$  to  $-11.6\text{‰}$ . The  $\delta^{13}\text{C}_{\text{CO}_2}$  in the groundwater was between  $-11.1$  and  $-18.5\text{‰}$ , which was calculated by (Eq. 6).

According to relative studies, the biogenic  $\delta^{13}\text{C}_{\text{CO}_2}$  was in the range between  $-16$  and  $-28\text{‰}$ , with the average of  $-22\text{‰}$ ; the atmospheric  $\delta^{13}\text{C}_{\text{CO}_2}$  was  $-7\text{‰}$ ; the mantle  $\delta^{13}\text{C}_{\text{CO}_2}$  was between  $-4$  and  $-11\text{‰}$ , with the average of  $-7\text{‰}$ ; the  $\delta^{13}\text{C}_{\text{CO}_2}$  degeneration of carbonate rocks was between  $-3$  and  $3\text{‰}$ , with the average of  $0\text{‰}$ . The calculated average  $\delta^{13}\text{C}_{\text{CO}_2}$  was  $-15.9\text{‰}$ , which demonstrated that the  $\text{CO}_2$  generated during the water-rock interaction was induced by factors of biogenetic, atmosphere, mantle and carbonate rocks degeneration. According to the above analysis, it was known that the  $\text{CO}_2$  in groundwater was multi-supplied.

From Table 6, the  $\delta^{13}\text{C}_{\text{CO}_2}$  in Yiliu hot spring was more positive than that of Yongkou hot spring. This again implied that Yiliu hot spring was under a more enclosed geological environment and the water-rock interaction was stronger than that of Yongkou hot spring. Furthermore, it explained that Yiliu hot spring started from NE-trending hills, ran through central Yiliu and outflowed in Wushui river basin.

**Table 6.**  $\delta^{13}\text{C}$  ratio characteristics in Yizhang geothermal groundwater

Number	T (°C)	$\delta^{13}\text{C}_{\text{HCO}_3^-}$ (‰)	$\delta^{13}\text{C}_{\text{CO}_2}$ (‰)	$\delta^{13}\text{C}_{\text{CO}_2}$ Average value
C444-2	44.8	-10.0	-16.3	-17.0
C444	35.7	-11.6	-18.5	
C443	41.5	-10.7	-17.3	
C443-1	43.5	-9.7	-16.1	
C439	42.9	-10.2	-16.7	
B374	27	-8.5	-16.2	-14.8
B373	20.7	-8.6	-16.8	
THL	20.5	-6.8	-15.0	
WQS	45.4	-4.8	-11.1	

## 5. Conclusions

In this paper, the characteristics of Yizhang groundwater were investigated. The hydrochemical characteristics in Yongkou hot spring and Yiliu hot spring were  $\text{HCO}_3\text{-SO}_4\text{-Ca}$  and  $\text{SO}_4\text{-Ca-Mg}$ , respectively. The water-rock interaction in the two regions was in the initial stage.

The hydrogeochemical characteristics changed in the order  $\text{HCO}_3\text{-Ca}$ ,  $\text{HCO}_3\text{-Ca}$ ,  $\text{HCO}_3\text{-SO}_4\text{-Ca}$ ,  $\text{SO}_4\text{-Ca-Mg}$  corresponding to surface water-underground cold water-Yongkou hot springs-Yiliu hot springs in Yizhang area, with the electrical conductivity increasing successively. Calcite and Dolomite were saturated while Gypsum and Fluorite were under saturated in the geothermal groundwater, and  $\text{SiO}_2$  in the geothermal groundwater were basically dissolved in Feldspar while the dissolution was not obvious in Chalcedony and Quartz.

According to the drift of  $\delta\text{D}-\delta^{18}\text{O}$  to the atmospheric rainfall lines, it was believed that the supply source of the geothermal groundwater was the rainfall and was formed by deep circulation heating. In addition, the supply path was short and the circulation of groundwater was fast. Yongkou and Yiliu hot springs shared the same geothermal supply source and had been formed in the same and relatively steady environment. The recharge height of geothermal field was between 695~1040m. It was confirmed that the source of underground hot water supply in Yizhang area was the Northeastward exposed carbonate area.

By the factors of biogenetic, atmosphere, mantle and carbonate rocks degeneration, the  $\text{CO}_2$  was released during the water-rock interaction in Yizhang groundwater. Yiliu hot spring was under a more enclosed geological environment and the water-rock interaction was stronger than that of Yongkou hot spring.

## Acknowledgements

This research was supported by the Guangxi Natural Science Foundation (No. 2018GXNSFAA294046 and No. 2017GXNSFAA198208), the National Key Research and Development Program of China (No. 2018YFC0604301), the National key Research and Development Program of China (No.2017YFC0406104) and the Geological survey project of China (No. DD20160303).

## References

- Bakari S.S., Aagaard P., Vogt R.D., (2013), Strontium isotopes as tracers for quantifying mixing of groundwater in the alluvial plain of a coastal watershed, South-Eastern Tanzania, *Journal of Geochemical Exploration*, **130**, 1-14.
- Barbato M., Cirillo L., Menditto L., Moretti R., Nardini S., (2017), Geothermal energy application in Campi Flegrei Area: The case study of a swimming pool building, *International Journal of Heat and Technology*, **35**, S102-S107.
- Caldera M., Ungaro P., Cammarata G., Puglisi G., (2018), Survey-based analysis of the electrical energy demand in Italian households, *Mathematical Modelling of Engineering Problems*, **5**, 217-224.
- Cannistraro M., Mainardi E., Bottarelli M., (2018), Testing a dual-source heat pump, *Mathematical Modelling of Engineering Problems*, **5**, 205-210.
- Craig H., (1963), The isotope geochemistry of water and carbon in geothermal areas, *Nuclear Geology in Geothermal Areas*, **20**, 17-53.
- Du J., Liu C., Fu B., (2005), Variations of geothermometry and chemical-isotopic compositions of hot spring fluids in the Rehai geothermal field, southwestern China, *Journal of Volcanology & Geothermal Research*, **142**, 243-261.
- Farnham I.M., Singh A.K., Stetzenbach K.J., (2002), Treatment of nondetects in multivariate analysis of groundwater geochemistry data, *Chemometrics & Intelligent Laboratory Systems*, **60**, 265-281.
- Ghasemkhani A., Farahat S., Naserian M.M., (2018), Thermodynamic investigation and optimization Tri-generation system for the provision of power, heating, and cooling: A case study of Zahedan, Iran, *International Journal of Heat and Technology*, **36**, 904-912.
- Giggenbach W., Sheppard D.S., Robinson B.W., (1994), Geochemical structure and position of the Waiotapu geothermal field, New Zealand, *Geothermics*, **23**, 599-644.
- Glavan I., Prelec Z., Pavkovic B., (2015), Modelling, Simulation and Optimization of Small-Scale CCHP Energy Systems, *International Journal of Simulation Modelling*, **14**, 683-696.
- Guo Q.H., Liu M., Li J., (2014), Acid hot springs discharged from the Rehai hydrothermal system of the Tengchong volcanic area (China): formed via magmatic fluid absorption or geothermal steam heating?, *Bulletin of Volcanology*, **76**, 868-869.
- Helstrup T., Jørgensen N.O., Banoeng B., (2007), Investigation of hydrochemical characteristics of groundwater from the Cretaceous-Eocene limestone aquifer in southern Ghana and Southern Togo using hierarchical cluster analysis, *Hydrogeology Journal*, **15**, 977-989.
- Kim S.T., O'Neil J.R., (2007), Equilibrium and nonequilibrium oxygen isotope effects in synthetic carbonates, *Geochimica et Cosmochimica Acta*, **61**, 3461-3475.
- Kuells C., Adar E.M., Udluft P., (2000), Resolving patterns of groundwater flow by inverse hydrochemical modelling in a semiarid Kalahari basin, *Tracers and Modelling in Hydrogeology*, **262**, 25-29.
- Majumdar N., Mukherjee A.L., Majumdar R.K., (2009), Mixing hydrology and chemical equilibria in Bakreswar geothermal area, Eastern India, *Journal of Volcanology & Geothermal Research*, **183**, 201-212.
- Nimick D.A., Moore J.N., Dalby C.E., (1998), The fate of geothermal arsenic in the Madison and Missouri Rivers, Montana and Wyoming, *Water Resources Research*, **34**, 3051-3067.
- Portugal E., Sandoval F., Barragan R.M., (2005), Isotopic ( $\delta^{18}\text{O}$ ,  $\delta\text{D}$ ) patterns in Los Azufres (Mexico) geothermal fluids related to reservoir exploitation, *Geothermics*, **34**, 527-547.
- Rissmann C., Christenson B., Werner C., (2012), Surface heat flow and  $\text{CO}_2$  emissions within the Ohaaki hydrothermal field, Taupo Volcanic Zone, New Zealand, *Applied Geochemistry*, **27**, 223-239.
- Ternik P., Buchmeister J., (2015), Buoyancy-induced flow and heat transfer of power law fluids in a side heated

- square cavity, *International Journal of Simulation Modelling*, **14**, 238-249.
- WHO, (1993), *Guidelines for Drinking-water Quality, Volume 1: Recommendations*, 2nd Edition, World Health Organization, Geneva, Switzerland, 1-26.
- Wang G., Wan J., Wang E., (2008), Late Cenozoic to recent transtensional deformation across the Southern part of the Gaoligong shear zone between the Indian plate and SE margin of the Tibetan plateau and its tectonic origin, *Tectonophysics*, **460**, 1-20.
- Wang G.L., Zhang W., Liang J.Y., (2017), Evaluation of geothermal resources potential in China, *Journal of the earth*, **38**, 448-459.
- Wang J.Y., (1996), Low-medium Temperature Geothermal System of Convective Type, *Earth Science Frontiers*, **3**, 96-102.
- Xu S.G., Guo Y.S., (2009), *Fundamental Geothermics*, In: Science Press, Beijing, 35-67.
- Yidana S.M., Ophori D., Banoeng B., (2008), Hydrogeological and hydrochemical characterization of the Voltaian Basin: the Afram Plains area, Ghana, *Environmental Geology*, **53**, 1213-1223.
- Zaher M.A., Saibi H., Nishijima J., (2012), Exploration and assessment of the geothermal resources in the Hammam Faraun hot spring, Sinai Peninsula, Egypt, *Journal of Asian Earth Sciences*, **45**, 256-267.
- Zhang B., Zhang J., Zhong D., (2012), Polystage deformation of the Gaoligong metamorphic zone: Structures,  $^{40}\text{Ar}/^{39}\text{Ar}$  mica ages, and tectonic implications, *Journal of Structural Geology*, **37**, 1-18.
- Zheng S.H., Hou G., (1983), A study of hydrogen and oxygen stable isotopes of atmospheric precipitation in China, *Chinese Science Bulletin*, **13**, 801-806.